Shear bands in a continuum model of foams: how a 3D homogeneous material may seem inhomogeneous in 2D

Sylvain Bénito, François Molino, Charles-Henri Bruneau, Thierry Colin, Cyprien Gay

Shear bands in a continuum model of foams : how a 3D homogeneous material may seem inhomogeneous in 2D

Sylvain BÉNITO
Université Bordeaux 1, INRIA Futurs projet MC2 et IMB, 351 Cours de la Libération, F–33405 TALENCE cedex, France

François MOLINO
Institut de Génomique Fonctionnelle, Department of Endocrinology, CNRS, UMR 5203, INSERM U661, Université Montpellier Sud de France, 141 Rue de la Cardonille, F–34094 MONTPELLIER cedex 05, France

Charles-Henri BRUNEAU and Thierry COLIN
Université Bordeaux 1, INRIA Futurs projet MC2 et IMB, 351 Cours de la Liberation, F–33405 TALENCE cedex, France

Cyprien GAY
Matière et Systèmes Complexes (MSC), CNRS UMR 7057, Université Paris Diderot–Paris 7, Bâtiment Condorcet, Case courrier 7056, 75205 Paris Cedex 13
(Dated: October 31, 2010)

We describe possible conditions for stationnary inhomogeneous flow behaviour (sheared and blocked bands) in a continuous mechanical model of a soft visco-elasto-plastic material such as a foam or a concentrated emulsion under controled shear rate conditions. Usually, the occurence of shear bands in a complex fluid is understood as resulting from a structural evolution of the material under shear, which leads from a theoretical perspective to a non-monotonic stationnary flow curve. Our mechanical model predicts a non-monotonic flow curve, but a priori without any intrinsic physical evolution *via* a parameter coupled to the flow such as concentration of entanglements. Nevertheless, we predict the appearence of shear bands. In our case, the non-monotonic flow curve and the appearence of shear bands result specifically from the tensorial character of the underlying model (2D or 3D). For a Couette flow, a 3D tensorial formalism allows us to introduce an additional relaxtion freedom for the system in the third direction, which affects the material fluidity.

PACS numbers: 47.57.Bc Foams and emulsions 83.10.Gr Constitutive relations - 83.80.Iz Emulsions and foams in Rheology - 83.50.AxSteady shear flows, viscometric flow

I. INTRODUCTION

It may seem paradoxical that a single material, when submitted to an uniform shear stress σ_{xy}, between two parallel plates or two coaxial cylinders, may be observed simultaneously in two distinct states in different regions of the flow. This observation has nevertheless become common since the early 1990s in a variety of complex fluids : so-called 'shear bands' appear and are stable [5, 10, 34], or sometimes fluctuate [1, 26, 39, 40]. Each band flows with a different shear rate. These bands are most of the time parallel with the plates [5].

The current understanding of these observations relies in general on two essential ingredients : (1) a structural evolution of the material under shear, and (2) a stress response which decreases as a function of the shear rate within a particular range. This decrease is the mechanical signature of the structural evolution and is the source of the mechanical instability that triggers the appearance of bands [27].

In polymer melts or entangled polymer solutions [42] and in entangled giant micelle solutions [27], the flow elongates the objects, which alters the apparent viscosity of the material (beware of wall slip [17]). The fact that this viscosity *goes down* is principally due to the average orientation of the objects in the shear flow.

In lyotropic lamellar phases, the transition can be associated with the reorganisation of the films in onion-like multilamellar vesicle systems [11, 12, 39, 40].

In micellar cubic crystals the transition consists in an ordering of the initial polycristal with specific planes becoming aligned with the plates [13, 14].

In the last two cases, no microscopic interpretation of the decrease in effective viscosity occuring during the transition is available.

In granular materials, surface flow is a particular case of shear bands. The lower band is in this case blocked (zero shear). No complete structural description is available. Nevertheless, it is admitted that the *dilatance* phenomenon, corresponding to the necessity for the grains to part a little bit in order to move past each other [36], generates a difference in volume fraction between the flowing region and the blocked one. This lower volume fraction tends to facilitate the flow in the flowing region even more as compared to the blocked region. When it is present, gravity is of course essential: it allows to determine the concentration profile [25].

In foams and emulsions, the situation is less clear. Shear bands were observed [9] But the role of solid walls in these effects is still controversial [20, 23, 24]. For these materials also, no complete structural description accounts for flow localization in a satisfactory manner. As for granular materials, dilatancy, which corresponds to a local change in water concentration ϕ, certainly plays an important role by easing the relative motion of bubbles. The structural disorder is also invoked as a parameter coupled to the flow [22]. In both cases, the local fluidity (ratio of the shear rate and the shear stress) is enhanced.

The model that we suggest does not incorporate any such ingredient. We write down the tensorial, three-dimensional equations of elasticity in the linear and non-linear regimes [3]. We show that it is sufficient to generate shear bands (a two-dimensional model is in fact also sufficient [35]). However, we know that a local plastic event results in an elastic redistribution of stress in the neighbourhood [15, 28]. In simple shear geometry, it favours flow localization [21, 32, 33]. In a statistical manner, it then raises the material fluidity in the neighbourhood [7] and generates a *non-local* material rheology. This non-local character had been observed in concentrated emulsions flowing in microfluidic channels [16]. These non-local effects are intrinsically present in our modelling since the underlying elastic propagators [7, 21, 32, 33] result directly from the elastic continuum medium equations that we use.

Under such conditions, how can the local material fluidity evolve in our model? As we shall see, it results from the fact that we take into account the tensorial character of the stress and the three dimensions of the material: in the example of a Couette flow, a local evolution of the material conformation in the direction perpendicular to the shear plane leads, from a 2D perspective, to a local fluidification.

A. A continuum medium model of foams and emulsions

In this paper, we describe the results obtained through the spatial simulation of a mechanical model of foams and concentrated emulsions. This model is contructed rigorously following the principles of continuum media mechanics [6]. Its main originality consists in writing the plastic and elastic laws in a very general form, and to combine these laws to the conservation relations. Thus, the plasticity formulation obeys such constraints as positivity of dissipation. The elasticity is written in a form valid up to large deformations, which are easily reached in such systems before plastic rearangments.

Thus, we introduce a framework in which constitutive laws and specific assumptions can be introduced and discussed afterwards.

Our main result: shear bands can emerge in a structurally homogeneous material under shear, only due to inhomogeneous distributions of the internal constraints present from the beguinning in the material. We demonstrate this for a physically very natural form of the elastic and plastic laws.

We restrain ourselves in this work to a strictly mechanical and thermodynamical formulation. The important problems related to the coupling between the rheological behaviour and the structure of the material are not discussed. This coupling is experimentally well documented in various complex fluids systems in which shear bands are *de facto* associated with structural transitions [27]. We ask a more restricted question: could *stationary* shear bands in foams and emulsions be accounted for using only inhomogeneous stress distributions present initially in the material?

B. Stationary flow curve and inhomogeneous flow

In our context, the main interest in studying a spatial model is to explore the conditions of appearance of inhomogeneous flow in the stationnary regime. It is important to understand that our local rheological model (constitutive law) must obey specific conditions for shear bands to appear and coexist. Indeed, in this situation, the *same material* submitted to the *same shear stress* σ_{xy} must be simultaneously *in two different deformation states*. A mathematical condition for this to be possible is the existence of an unstable zone in the local flow curve of the material [4, 34, 41], which corresponds to the non-linearity of the constitutive law.

In the case of foams, nevertheless, such an unstable portion in the flow curve itself does not exist: how can shear bands with different shear rates coexist?

Foams and emulsions are instances of yield stress fluids, so that there exists a minimal stress σ_{xy} (that we denote by σ_y) below which no stationary flow occurs. Now when we shear the material, imposing the *shear rate*, the material *has* to flow, even for very small $\dot{\gamma}$. The intrinsic flow curve thus possesses an extrapolation in stress when $\dot{\gamma} \to 0$. Let's denote it by σ_d. Note that σ_y and σ_d pertain to the local rheology curve, not to the effective stationary curve as can be measured for example in a rheometer. In this discussion the flow is *homogeneous*. But the relative values of σ_d and σ_y, pertaining to the local flow curve, will give us hints about possible conditions for shear banding.

Let us now consider the result of a measurement made on a sample of this material, sheared in a Couette cell under imposed shear rate. If $\sigma_d > \sigma_y$, all parts of the sample will flow, even at low shear rates, since the corresponding stress is necessarily everywhere greater than the yield stress. As mentionned before, since the flow curve has no intrinsic instability for higher $\dot{\gamma}$ values, no mechanism is available for shear banding.

The situation is different if $\sigma_d < \sigma_y$. If we put on the same graph the yield stress σ_y and the intrinsic stationary flow curve (figure 1), it is immediately apparent that

this configuration allows for the coexistence of zones underging shear at rates $\dot{\gamma} \geq \dot{\gamma}_c$, and of blocked zones at zero shear remaining in the elastic regime. The mechanism is essentially the same as in the classical case of instability in the flow curve (see figure 1). Of course, as soon as $\dot{\gamma} > \dot{\gamma}_c$ all regions flow, since $\dot{\gamma} > \dot{\gamma}_c$ implies that *some* regions flow *faster* than $\dot{\gamma}_c$. The stress in these regions, as given by the flow curve, has to be above the yield stress σ_y. And since the stress is the same in the entire material, all regions support a stress greater than σ_y and no region can be blocked.

C. Extra dynamic variables?

But is the situation where $\sigma_d \neq \sigma_y$ actually possible? The answer is known to be yes. The usual explanation of such a flow curve is to invoque an internal extra variable (of a structural nature in general) which is coupled to the flow. As an example, in a simplified vision, this extra parameter can be in one of two states: flowing and non-flowing. Thus the stationnary curve extrapolating to σ_d at low $\dot{\gamma}$, and the yield stress value σ_y correspond in reality to two different materials. One of the interests of our work is to elaborate a situation where $\sigma_d \neq \sigma_y$ is possible without any extra structural parameter. As we will see, if one writes a fully tensorial formulation for the constitutive equation, the shear flow curve $\sigma_{xy}(\dot{\gamma})$ can be of the $\sigma_d < \sigma_y$ sort. The extra components of the stress σ_{xx} and σ_{zz} will qualitatively play the same role as an extra structural variable in changing the local nature of the material. Their initial distribution in the material will thus be of primary importance in predicting shear bands.

Despite some similarities, the analogy with systems characterised by unstable flow curves has some limitations. In the case of yield stress fluids, there is no unstable range in $\dot{\gamma}$, which would *impose* phase separation between two phases at different flow rates. Shear bands are *possible* but not *necessary*. Also, no lever rule-like criterion can exist to select the relative fraction of the different bands, as have been argued in some fluid systems [31, 34]. It is the *material history* which will lead to a particular flow profile. We will see that the initial distribution of stress in the material will determine the band structure.

The paper is organised as follows. We first describe our continuous model, specifying both its local rheological behaviour and the complete set of partial differential equation in 3D+time. We then proceed to analyse the rheological law in more detail, to show how it can predict, under some particular intitial conditions, shear bands (blocked bands in this case). We then present the results of spatial simulations which confirm the band existence as predicted by the rheological law. We analyse the band structure dependence on the different rheological parameters of the system.

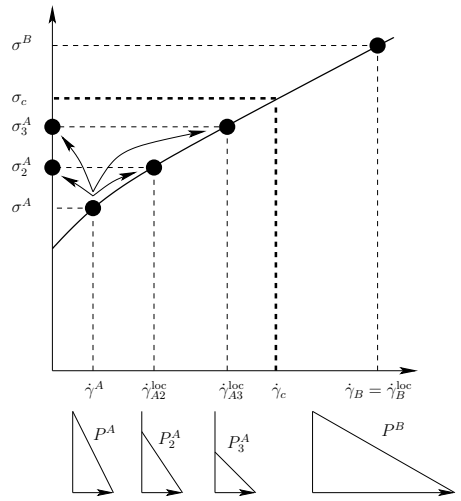

FIG. 1: Typical form of a stationnary flow curve giving the dependence of the shear stress on the local shear rate. σ_y is the yield stress as measured under imposed stress, and $\dot{\gamma}_c$ the corresponding shear rate. A macroscopic shear rate $\dot{\gamma}^A$ smaller than $\dot{\gamma}_c$ will not necessarily lead to a homogeneous velocity profile P^A, with the expected stress σ^A: the flow can separate into a blocked region and a flowing region (profiles P_2^A or P_3^A). The local shear rate is then faster ($\dot{\gamma}_{A2}^{\rm loc} > \dot{\gamma}^A$ and $\dot{\gamma}_{A3}^{\rm loc} > \dot{\gamma}^A$), which corresponds to a higher stress ($\sigma_2^A > \sigma^A$ and $\sigma_3^A > \sigma^A$). Besides, for an average shear rate $\dot{\gamma}^B$ greater than $\dot{\gamma}_c$, the flow is homogeneous again, which corresponds to the expected stress σ^B (greater than σ_y).

II. CONSTRUCTING A CONTINUUM MODEL

Our local rheological model [3] is based on a general nonlinear description of elasticity and plasticity. Indeeds materials such as foams can locally undergo large elastic deformations — located far from the linear regime corresponding to small deformations — before plastic flow occur [8, 43].

A. General local rheological laws

The relevant framework to describe elastic stresses in a flowing material is the Eulerian one, whether this material possesses elastical properties or not. Indeed, during the flow of a foam or an emulsion, even though elastic stresses exist, any reminiscence of a *reference state* is lost continuously due to plasticity. The Lagrangian description, which is based on maintaining the correspondance with such an intial state of reference, is formally equivalent, but less adapted conceptually and numerically.

Thus we attach the variables describing the material to a spatial grid (x, y, z), and they correspond to an instantaneous and local description in space.

In this framwork, only two variables are relevant in a strictly mechanical context: the local velocity gradient $\nabla\vec{v}(x, y, z)$ and the local deformation state stored in the

material [3], as described in continuum mechanics by the Finger tensor $B(x, y, z)$ [6].

In this section, we describe our local rheological model. Note that in this local context, the global tensor $\nabla\vec{v}$ itself has to be considered as an independent local three-dimensional tensorial variable, just as B, not as the spatial gradient of a velocity field. Only when we will turn to the description of a spatial system, see section IV, will the vector field $\vec{v}(x, y, z)$ be introduced. Meanwhile, tensors $\nabla\vec{v}$ and B will thus be the two variables of our local tensorial model.

Elasticity depends on the deformation according to the following relation, the most general one compatible with the symmetry constraints in three dimensions [3]:

$$\sigma = a_0\,\mathrm{I} + a_1\,B + a_2\,B^2, \tag{1}$$

where a_0, a_1 and a_2 are scalar functions of the invariants of the Finger tensor B.

Turning to plasticity, we only assume that every event of plastic relaxation is *aligned* with the stored deformation. The plastic creep D_{p}^B should thus be similarly aligned. The most general form compatible with the symmetry constraints is then:

$$D_{\mathrm{p}}^B = \bar{b}_0\,\mathrm{I} + \bar{b}_1\,B + \bar{b}_2\,B^2, \tag{2}$$

where $\bar{b}_0$, $\bar{b}_1$ and $\bar{b}_2$ are again scalar functions of the invariants of the Finger tensor B.

To complete the model, we gather together in a global viscosity term all the dissipative phenomena which are present even in the absence of any plastic event in the foam. They occur for example at small scales: flows in films squeezed between bubbles or in Plateau borders. We simplify the description in selecting a Newtonian average viscosity for these local dissipative phenomena. The list of contributions to the stresses in the material is thus closed. We have:

$$\sigma = a_0\,\mathrm{I} + a_1\,B + a_2\,B^2 + \frac{\eta_s}{2}(\nabla\vec{v} + \nabla\vec{v}^{\mathrm{T}}). \tag{3}$$

To take into account the incompressible character of foams and emulsions, we add an extra kinematic constraint of strict volume conservation $\det(B) = 1$. Refering to [3] for further details, we take it into account by using only the deviatoric part of the stress:

$$\bar{\sigma} = \mathrm{dev}(\sigma) = \sigma - \frac{\mathrm{I}}{d}\mathrm{tr}(\sigma). \tag{4}$$

The same constraint on plasticity gives the general form [3]:

$$D_{\mathrm{p}}^B = B\cdot\mathrm{dev}(f(B)) = b_1\,B\cdot\mathrm{dev}(B) + b_2\,B\cdot\mathrm{dev}(B^2), \tag{5}$$

where the scalar prefactors b_1 and b_2 are isotropic, and thus depend on the invariants of tensor B.

In what follows, we will use a completely equivalent form of tensor D_{p}^B which manifests more clearly the positive character of the dissipation (see the discussion in [3]):

$$D_{\mathrm{p}}^B = \frac{\mathcal{A}(B)}{\tau}\,B\cdot\mathcal{G}(B) \tag{6}$$

where $\mathcal{A}(B)$ is a scalar isotropic function of B, τ the characteristic time of the dissipative processes; moreover:

$$\mathcal{G}(B) = \frac{\mathrm{dev}\left[\mathcal{P}(B)\cdot\mathrm{dev}(\sigma)\right]}{\mathrm{tr}\left[\mathcal{P}(B)\cdot\mathrm{dev}(\sigma)\cdot\mathrm{dev}(\sigma)\right]}, \tag{7}$$

with $\mathcal{P}$ is a function of the form $\mathcal{P}(B) = b(B)\,B^{-2} + (1 - b(B))\,B^2$ [3], where b is an isotropic function. In this expression, the total dissipation per unit volume is $\mathcal{A}(B)$.

Eventually one gets the complete rheological model:

$$\frac{\mathrm{d}B}{\mathrm{d}t} - \nabla\vec{v}\cdot B - B\cdot\nabla\vec{v}^{\mathrm{T}} = -2\,D_{\mathrm{p}}^B, \tag{8}$$

$$D_{\mathrm{p}}^B = \frac{\mathcal{A}(B)}{\tau}\,B\cdot\mathcal{G}(B), \tag{9}$$

$$\sigma = a_0\,\mathrm{I} + a_1\,B + a_2\,B^2 + \frac{\eta_s}{2}(\nabla\vec{v} + \nabla\vec{v}^{\mathrm{T}}). \tag{10}$$

B. Complete spatial model

As for any local rheological model, the previous equations must be complemented by field equations which express force balance and mass conservation:

$$\nabla\cdot\bar{\sigma} + \rho\,\vec{f} = \rho\frac{\mathrm{d}\vec{v}}{\mathrm{d}t} + \vec{\nabla}\,p, \tag{11}$$

$$\frac{\partial\rho}{\partial t} + \nabla\cdot(\rho\,\vec{v}) = \frac{\mathrm{d}\rho}{\mathrm{d}t} + \rho\,\mathrm{tr}\frac{1}{2}(\nabla\vec{v} + \nabla\vec{v}^{\mathrm{T}}) = 0, \tag{12}$$

where $\vec{f}$ represents the external forces (per unit mass), and ρ is density. The incompresibility constraint gives here

$$\nabla\cdot\vec{v} = \mathrm{tr}\frac{1}{2}(\nabla\vec{v} + \nabla\vec{v}^{\mathrm{T}}) = 0. \tag{13}$$

As a result, the density ρ is simply transported by the flow: $\mathrm{d}\rho/\mathrm{d}t = 0$. In the remaining of this work, we furthermore assume that the density is homogeneous, hence it remains constant.

Last assumption: we restrict ourselves to the Stokes regime, where inertial terms are all negligible in the mass conservation equation. Thus one obtains:

$$\nabla\cdot\bar{\sigma} = \vec{\nabla}\,p. \tag{14}$$

The complete system of equations that we have to integrate numerically is thus:

$$\frac{\mathrm{d}B}{\mathrm{d}t} - \nabla\vec{v}\cdot B - B\cdot\nabla\vec{v}^{\mathrm{T}} = -2\,D_{\mathrm{p}}^B, \tag{15}$$

$$D_{\mathrm{p}}^B = \mathcal{A}(B)\,B\cdot\mathcal{G}(B), \tag{16}$$

$$\bar{\sigma} = \mathrm{dev}\left\{ a_0\,\mathrm{I} + a_1\,B + a_2\,B^2 + \frac{\eta_s}{2}(\nabla\vec{v} + \nabla\vec{v}^{\mathrm{T}}) \right\}, \quad (17)$$

$$\nabla\cdot\bar{\sigma} = \vec{\nabla}\,p, \quad (18)$$

$$\mathrm{tr}\frac{1}{2}(\nabla\vec{v} + \nabla\vec{v}^{\mathrm{T}}) = 0. \quad (19)$$

The initial conditions that must be specified to solve the above system may merely consist in the values of tensor B over the entire sample. Indeed, the value of the velocity field can be derived therefrom using Stokes' equation (15).

C. Selection of a particular form of elasticity and plasticity

1. Elasticity: Mooney-Rivlin model

We have selected a usual form of incompressible elasticity which has been demonstrated to describe to a good approximation the nonlinear elastic behaviour of foams [18, 19]: Mooney-Rivlin elasticity. The corresponding elastic energy can be written [6]:

$$\rho\,E(B) = \frac{k_1}{2}(\mathrm{I}_B - 3) + \frac{k_2}{2}(\mathrm{II}_B - 3) \quad (20)$$

where

$$\mathrm{I}_B = \mathrm{tr}(B) \quad (21)$$

$$\mathrm{II}_B = \frac{1}{2}[\mathrm{tr}^2(B) - \mathrm{tr}(B^2)] = \mathrm{tr}(B^{-1}) \quad (22)$$

Going back the coeficients of Eq. (1), this corresponds to the following expressions:

$$a_1 = k_1 + k_2\,\mathrm{I}_B \quad (23)$$

$$a_2 = -k_2 \quad (24)$$

Following previous work refs. [18, 19], we express the values of k_1 and k_2 using an elastic modulus G and an interpolation parameter a as follows:

$$k_1 = aG \quad (25)$$

$$k_2 = (1-a)G. \quad (26)$$

In the foam modelling litterature, a value $a = \frac{1}{7}$ is sometimes recommended [18, 19]. Keeping in mind our perspective of discussing the conditions for the appearance of shear bands depending on parameter values, in sections III and beyond, we prefer to keep the parameter a free, although we remain in the framework of the Moonley-Rivlin elasticity.

2. Plasticity: yield stress fluid

The particular form of plasticity explored in this work is based on a nonlinear threshold-like behaviour. Locally, the plastic reorganisation events only occur in the material when the stored elastic deformation reaches a critical value. We express this transition with a function $W_y(B)$ which vanishes linearly at the threshold:

$$W_y(B) = 0, \quad (27)$$

with, in our case, $W_y(B) = E(B) - K$, where E is the stored elastic energy, and K a constant. In simple shear from a relaxed state, σ_y is the threshold stress: function W_y vanishes.

From the point of view of the plastic deformation rate tensor D^B_{p}, we have the following expression 6, taking for $\mathcal{A}(B)$:

$$\mathcal{A}(B) = (E(B) - K)\,\Theta(E(B) - K), \quad (28)$$

where $\theta(x) = 1$ when $x \geq 0$ and $\theta(x) = 0$ elsewhere.

We also set the following form for the polynom:

$$\mathcal{P}(B) = bB^{-2} + (1-b)B^2. \quad (29)$$

with b between 0 and 1. Our final set of equations is thus:

$$\frac{\mathrm{d}B}{\mathrm{d}t} - \nabla\vec{v}\cdot B - B\cdot\nabla\vec{v}^{\mathrm{T}} = -2\,D^B_{\mathrm{p}}, \quad (30)$$

$$D^B_{\mathrm{p}} = \frac{E(B) - K}{\tau}\,\Theta(E(B) - K)\,B\cdot\mathcal{G}(B), \quad (31)$$

$$\begin{aligned}\bar{\sigma} = \mathrm{dev}(\sigma) = \mathrm{dev}\,\{&(a\,G + (1-a)\,G\,\mathrm{tr}(B))\;B \\ &- (1-a)G\,B^2 \\ &+ \frac{\eta_s}{2}(\nabla\vec{v} + \nabla\vec{v}^{\mathrm{T}})\Big\}, \end{aligned} \quad (32)$$

$$\nabla\cdot\bar{\sigma} = \vec{\nabla}p. \quad (33)$$

$$\mathrm{tr}\frac{1}{2}(\nabla\vec{v} + \nabla\vec{v}^{\mathrm{T}}) = 0. \quad (34)$$

3. Physical parameters and rheological model

A non-dimensional form of the previous system is usually used, in order to emphasize certain quantities which are physically relevant. Stress σ is put in units of the elastic modulus G, and time is replaced by the non dimensional variable $\mathcal{T} = \dot{\gamma}\,t$. Equations (30) and (32) then read:

$$\frac{\mathrm{d}B}{\mathrm{d}\mathcal{T}} - \nabla\vec{v}\cdot B - B\cdot\nabla\vec{v}^{\mathrm{T}} = -2\,\mathrm{We}D^B_{\mathrm{p}}, \quad (35)$$

$$\bar{\sigma} \;=\; \mathrm{dev}\Big\{ (a \,+\, (1-a)\,\mathrm{tr}(B))\; B \\ -\,(1-a)\,B^2 + \frac{1}{\alpha}(\nabla\vec{v} + \nabla\vec{v}^{\mathrm{T}})\Big\}, \qquad (36)$$

with We $= \dot{\gamma}\tau$ et $\alpha = \frac{2\,G}{\eta\,\dot{\gamma}}$. In equation (31), K is replaced by $\mathcal{K} = K/G$. The parameters of our rheological model are thus $\mathcal{K}$, α, We, with the scalars a (Mooney-Rivlin parameter) and b (defining the tensorial form of the plasticity $\mathcal{G}(B)$).

D. Simple shear flow

In the remaining of this work, we address specifically the question of shear banding. For this purpose, we consider only simple shear flows. The velocity is oriented along axis x and varies along along axis y. The only non-zero component of the velocity gradient $\nabla\vec{v}$ is then $\partial v_x/\partial y$. The entire system and flow are invariant along x and z. Besides, the force balance given by Eq. (33) then implies that σ_{xy} and σ_{yy} are homogeneous at all times.

III. HOMOGENEOUS FLOW BEHAVIOUR

A. Model analysis and shear banding criteria

As long as the flow in the material is homogeneous, the local rheological model will describe it. We begin by showing the corresponding typical flow curve (fig. 2). Note that this flow curve is obtained under applied shear rate conditions.

As can be observed, the conditions described in the introduction for the appearance of shear bands are fulfilled: stress σ_d is smaller than the static yield stress σ_y. In the shear rate range between 0 and $\dot{\gamma}_c$, the system has the possibility to split the average shear rate $\dot{\gamma}$ in different proportions of blocked and flowing bands.

Thus, in the homogeneous case, we can calculate from the local rheological model, and for any values of the parameters We, α, $\mathcal{K}$, a, and b, the static and dynamic thresholds, σ_y and σ_d, and the critical shear rate $\dot{\gamma}_c$. Following the line of reasoning developped in the introduction, we can then predict the range of imposed shear rates $[0,\, \dot{\gamma}_c]$ inside which shear bands are *possible*.

The value of σ_y can be obtained easily by simulating the system in the elastic regime ($D^B_{\mathrm{p}} = 0$) up to the threshold ($W_y(B) = 0$), which corresponds to a state of the system characterized by eigenvalues β^y_1 and β^y_2 of tensor B, a state for which σ_y can be calculated.

One could then obtain the different stationary state values of the shear stress independently by continuing the simulation beyond the threshold in the plastic regime for each value of $\dot{\gamma}$, waiting for the stationnary value of the system ($\mathrm{d}B/\mathrm{d}t \approx 0$). The dynamic threshold σ_d would then correspond to the limit of σ_{12} for small $\dot{\gamma}$. The critical shear rate $\dot{\gamma}_c$ would be obtained when the stress applied to the system in the stationary state would precisely correspond to the plastic threshold: $\sigma^{\mathrm{stat}}_{12}(\dot{\gamma}_c) = \sigma_y$. Such a procedure is natural, but requires successive simulations of the system for a large number of $\dot{\gamma}$ values.

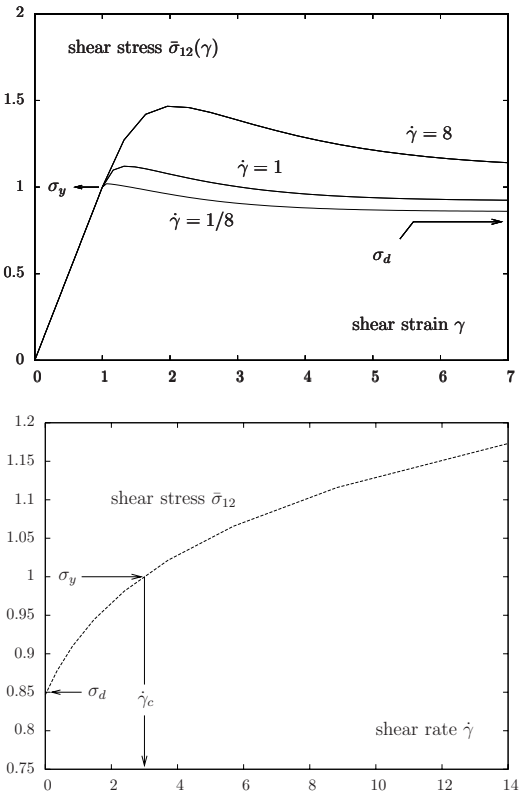

FIG. 2: Top: typical stationary flow curve. Points corresponding to σ_d, σ_y and $\dot{\gamma}_c$ are reported on the curve. Bottom: stress time evolution for different imposed shear rates below or above $\dot{\gamma}_c$.

We have used a more direct approach [3] to obtain σ_d and $\dot{\gamma}_c$ (see Appendix). This method relies on the description of the evolution of the system (as represented in figure 16) in terms of independent eigenvalues β_1 and β_2 of tensor B.

With the help of this procedure, the three observables which are important for the prediction of shear bands, σ_y, σ_d, and $\dot{\gamma}_c$, are obtained directely without the need for simulating separately all the points along the stationary flow curve.

B. Results

In this section, we want to describe, within the parameter space ($\mathcal{K}$, α, We, a, b) the regions inside which shear bands are possible. These domains will be represented through sections in four different planes: (α, We),

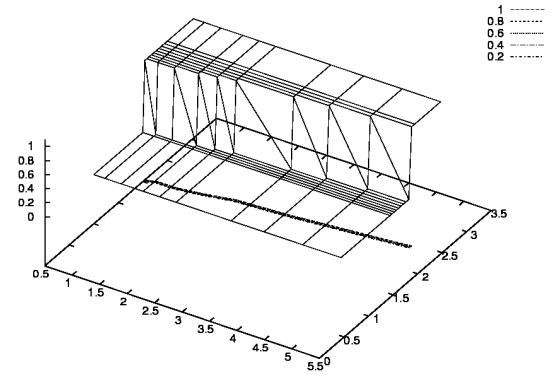

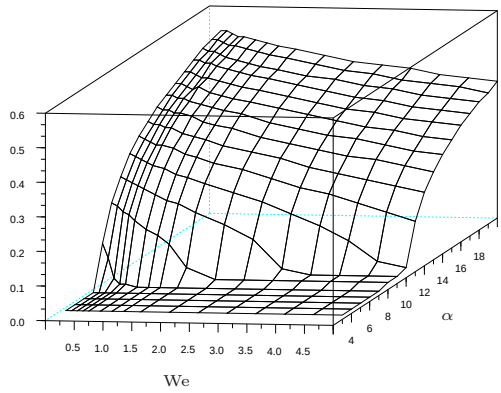

FIG. 3: Possibility (value 1) or not (value 0) to have a blocked band as a function of α between 1 and 3 and We between 0.5 and 5 (with $\mathcal{K} = 1$, $a = b = 0.5$).

FIG. 4: Width of the blocked band as a function of α between 3 and 20 and We between 0.2 and 5 (with $\mathcal{K} = 1$, $a = b = 0.5$).

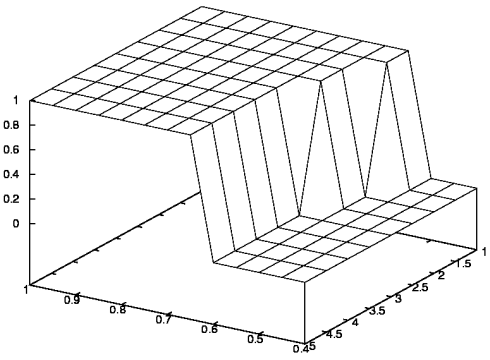

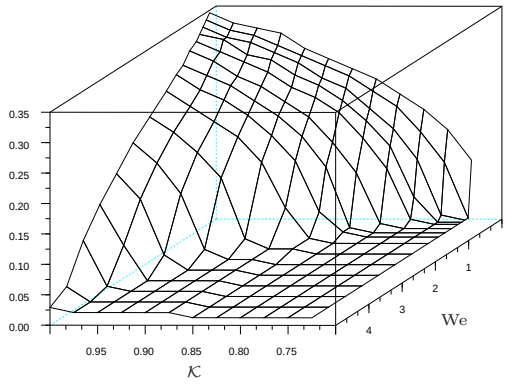

FIG. 5: Possibility (value 1) or not (value 0) to have a blocked band as a function of $\mathcal{K}$ between 0.4 and 1 and We between 1 and 5 (with $\alpha = 10$, $a = b = 0.5$).

FIG. 6: Width of the blocked band as a function of $\mathcal{K}$ between 0.725 and 1 and We between 0.2 and 5 (with $\alpha = 10$, $a = b = 0.5$).

($\mathcal{K}$,We), (a, b) and (α, $\mathcal{K}$).

The five parameters have a rather straightforward rheological interpretation, which are summarised in figure 15. Parameters α^{-1} and We are proportional to the imposed shear rate, $\mathcal{K}$ to the yield stress. Moreover, each α^{-1} and We is proportional to one of the viscosities of the medium.

In figure 3, one can see that in the (α, We) plane, shear bands are only possible for values of α large enough (between 3 and 10 depending on We values). Indeed for large values of α both shear rate and viscosity decrease. These conditions are physically intuitive for the appearance of shear bands, since they appear for small velocities and their range will be all the more extended that the slope at the origin of the flow curve is small. Moreover, bands appear more easily for small values of We, for the same reasons (small velocities).

In the ($\mathcal{K}$, We) plane, bands should be predicted for small values of We (again due to the small velocities), and for large values of $\mathcal{K}$. Indeed, in that case the static threshold is large which favours bands since they are possible *below* this threshold (figure 5).

The interpretation is similar in the (α, $\mathcal{K}$) plane, since α is inversely proportional to the shear velocity (figure 7).

Finally, in the (a, b) plane, one is confronted with 3D effects which are difficult to discuss in intuitive terms (figure 11). The way the elasticity (parameter a) and the plastic deformation rate (parameter b) are coupled in a tensorial way affects the critical rate $\dot{\gamma}_c$ and can be enough to eliminate all possibilities of shear bands.

IV. STATIONARY FLOW REGIMES

The discussion in the previous paragraphe only provides *necessary* conditions for the appearance of shear bands. In the 1D simulations that will be discussed in the present Section [2], flow inhomogeneities will indeed emerge.

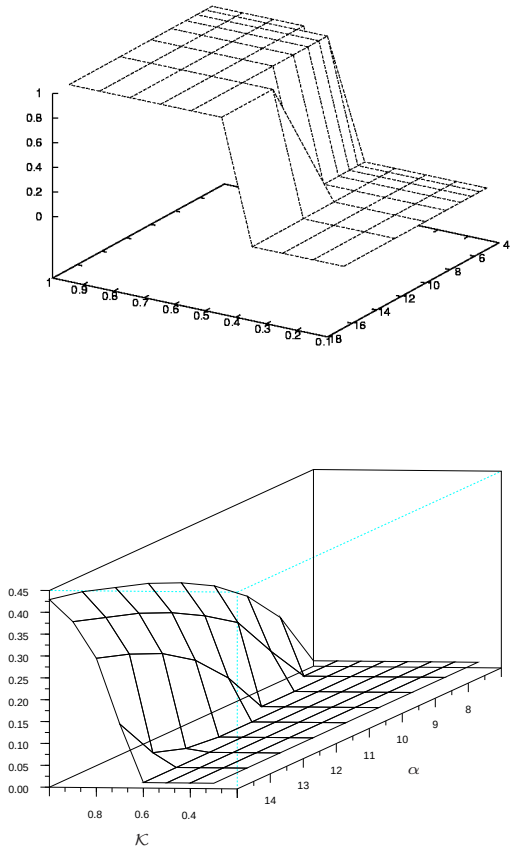

FIG. 7: Possibility (value 1) or not (value 0) to have a blocked band as a function of α between 7 and 15 and $\mathcal{K}$ between 0.1 and 1 (with We $= 1$, $a = b = 0.5$).

FIG. 8: Width of the blocked band as a function of α between 7 and 15, and $\mathcal{K}$ between 0.3 and 1 (with We $= 1$, $a = b = 0.5$).

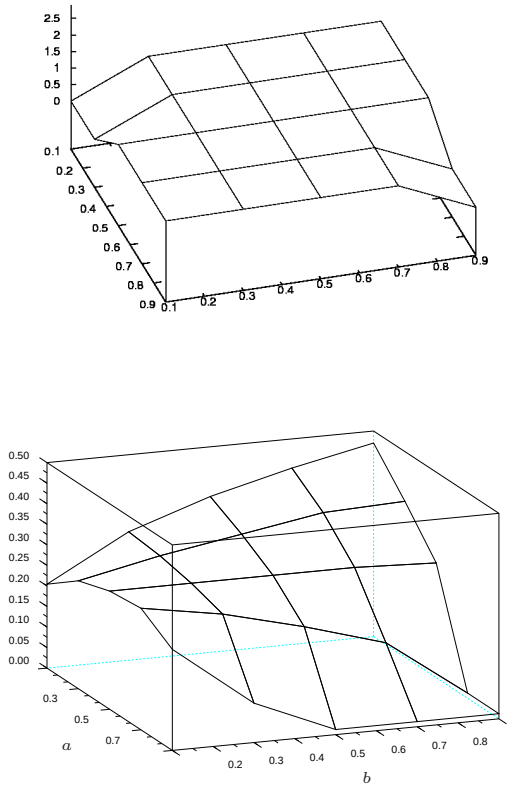

FIG. 9: Possibility (value 1) or not (value 0) to have a blocked band as a function of a between 0.1 and 0.9 and b between 0.1 and 0.9 (with $\alpha = 2.5$, We $= \mathcal{K} = 1$). Note that for $\alpha = 10$, all values of a and b lead to the possibility to have a blocked band (value 1).

FIG. 10: Width of the blocked band as a function of a between 0.1 and 0.9, and b between 0.1 and 0.9 (with $\alpha = 10$, We $= \mathcal{K} = 1$).

Now, the model that we simulate only contains material parameters that *homogeneous* in the sample. Hence, if the *initial conditions* of the flow are also homogeneous, the entire evolution will remain homogeneous. Although performing a 1D simulation as a set of partial differential equations, we would obtain the exact same results as in the previous Section.

In other words, since the parameters of the model do not vary in space, shear bands can only appear if initial conditions are, in one way or another, inhomogeneous.

Of course, as mentioned in the Introduction, inhomogeneities could appear in a natural way through an extra state variable coupled to the flow, such as the concentration. This variable could then vary in space and be coupled to the flow. Concerning concentration (a conserved variable), let us mention dilatancy phenomena, imagined for foam [37, 44], observed experimentally [29] and interpreted in a geometrical manner [30, 38]. Alignement (a non-conserved variable) is another possibility. It has been invoked in the case of wormlike micelle or rigid rod solutions [31].

Here, we focus on inhomogeneous static stress initial conditions, without invoking additional variables, and we will show that they can induce the appearance of persistent inhomogeneities in the flow profile.

The reason for which these initial stress inhomogeneities can induce the appearance of blocked bands can be qualitatively undestood by considering the flow threshold $\mathcal{K}$. Indeed, the stresses generated by the shear combine with the initial stress distribution. Depending on its orientation, the initial stress thus precipitates or delays the triggering of the plastic flow.

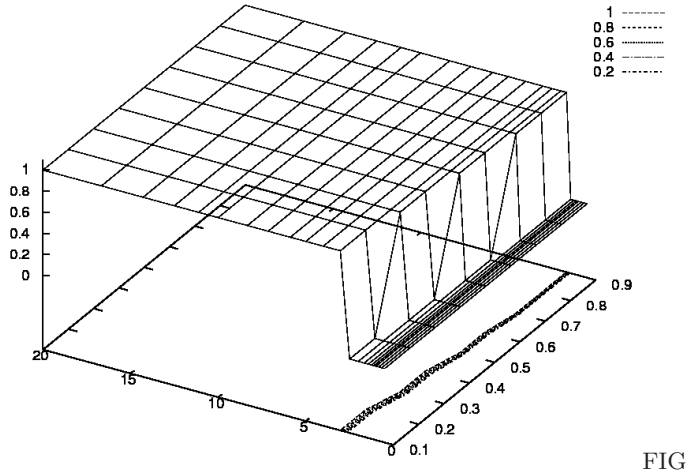

FIG. 11: Possibility (value 1) or not (value 0) to have a blocked band as a function of b between 0.1 and 0.9 and α between 1 and 20 (with $a = \frac{1}{7}$, We $= \mathcal{K} = 1$).

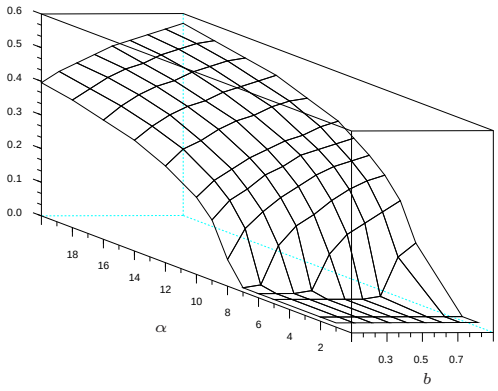

FIG. 12: Width of the blocked band as a function of b between 0.1 and 0.9, and α between 1 and 20 (with $a = \frac{1}{7}$, We $= \mathcal{K} = 1$).

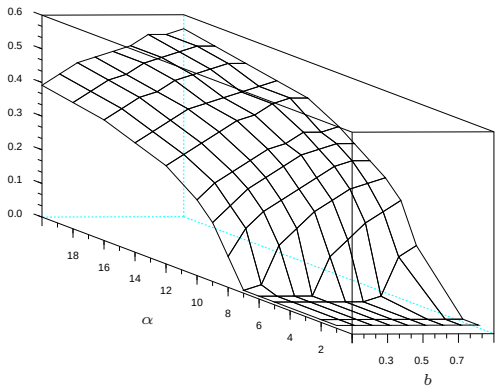

FIG. 13: Width of the blocked band as a function of b between 0.1 and 0.9, and α between 1 and 20 (with $a = \frac{1}{7}$, We $= \mathcal{K} = 1$).

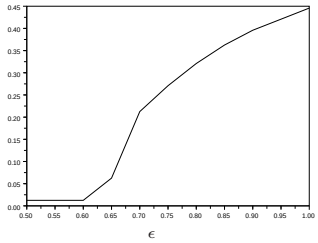

FIG. 14: Width of the blocked band as a function of ϵ (with $\alpha = 16$, We $= \mathcal{K} = 1$, $a = b = 0.5$).

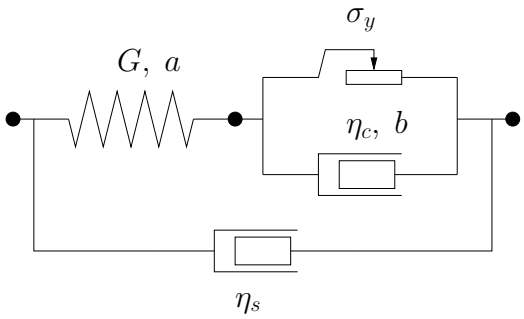

FIG. 15: A simplified (scalar) picture of the main rheological parameters. G represents the elastic modulus and a the relative weight of the tensorial components of the elastic deformation, see Eqs. (25) and (26). The quantities σ_y and η_c constitute a scalar representation of the creep defined by $D_{\rm p}^B$, and parameter b is the equivalent of a for creep, see equation (29). Finally, η_s is a viscosity that is independent of creep. $\alpha = \frac{2\,G}{\eta\,\dot\gamma}$ thus expresses the ratio between the elastic stress and the viscous stress, and $\mathcal{K} = K/G$ the threshold in units of the elastic modulus. As for We $= \dot\gamma\tau$, it expresses the relation between the characteristic time of the imposed shear rate $\dot\gamma$ and that of the relaxation in the vicinity of the threshold, τ (see Eq. 31).

A. Initial inhomogeneous stress distribution

First, the existence of stress inhomogeneities stored in the system before it is set into motion is physically well motivated. For instance, introducing a foam sample into an apparatus requires non-homogeneous flows. Inhomogeneous stresses will build up in the sample very likely, except if particular care is taken, such as a slow, *in situ* drying of an initially wet foam.

We will always assume that the initial state is at rest, that is, that the elastic stresses are at equilibrium in the sample. However, even when this equilibrium is imposed, there exist a large set of initial spatial distributions of stress. For example, if the system is invariant in the xz plane of the shearing walls, some components of the

stress must be homogeneous. That is the case for σ_{xy}, σ_{yy} and σ_{yz}. The other stress components, however, can freely vary as a function of y as long as they remain constant in each xz plane. It thus corresponds to a 1D inhomogeneity in the direction of the velocity gradient.

In this paragraph, we examine a very simple case of initial condition, where only the σ_{xx} component varies:

$$\sigma_{xx} = 1 - 4\epsilon\,|y(1-y)|, \tag{37}$$

all other components being identically zero.

In practice, in order to prepare a sample in such a state, one must compress the foam in a non-homogeneous manner. Typically, a block of foam with a trapezoidal shape is forced to take a rectangular shape.

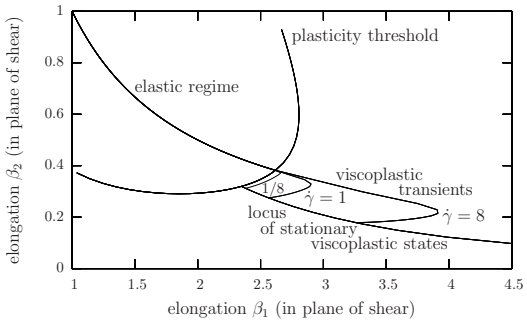

FIG. 16: Form of the stored elastic deformation in the course of an experiment and in the stationary regime, for three different values of the shear rate $\dot\gamma$. The axes are the first two eigenvalues, β_1 and β_2, of tensor B.

B. Characterizing the inhomogeneous flows

A typical sequence of velocity profiles obtained in our numerical simulations displays as follows. The velocity profile is initially homogeneous. It remains homogeneous as long as the entire sample is in the elastic regime. The regions where the initial stress is the highest in the direction of the applied deformation reach the threshold first. The average shear rate being constant, this onset of creep leads both to a higher shear rate in the creeping regions and to a lower one in the others. The high shear rate then induces the saturation of the stress due to creep, and the shear becomes blocked in the region below the threshold. In the stationary regime, a blocked band coexists with a sheared band at the same shear stress.

In the corresponding transient regime, non-trivial phenomena may appear, especially at the boundary of the blocked zone. Transient negative local shear rates are observed due to stored elastic stresses.

Let us now address the characteristics of the stationary velocity profile, again from the behaviour of the local rheological model.

The first feature of interest is that in the flowing regions, the velocity profile is linear, that is, the shear rate is uniform. That can be understood in the following manner. All the regions which, in the stationary state, respond through a non-zero shear rate, correspond to a point located on the stationary flow curve in the β_1-β_2 diagram of figure 16. Each point of this curve corresponds to a different shear stress. Thus, since each layer of the flow undergoes the same shear stress, they all actually correspond to the same point on the curve and thus respond through the same shear rate.

A second feature results from the fact that in space, while σ_{xy} and σ_{yy} are continuous, σ_{xx} and σ_{zz} can perfectly be discontinuous. That is precisely the case at the boundary between a shear and a blocked region. This is the flow counterpart of the discontinuity in the β_1-β_2 diagram, between the points below the threshold and the point with a stationary shear rate that corresponds to the flowing region. Actually, the only coupling between the different layers comes from the fact that *(i)* σ_{xy} and σ_{yy} must be every where the same, and *(ii)* the integral of $\dot\gamma$ over the gap thickness is fixed by the imposed wall velocity. As a consequence, in an inhomogeneous flow, the organisation of the blocked and flowing layers is not unique: any permutation of the layers is actually possible. Again, initial conditions decide upon the particular structure adopted by the flow. Two initial conditions corresponding to permutated layers would lead to the same permutation in the stationary flow structure.

C. Parameters affecting the existence of blocked bands

1. 1D results

With these 1D simulations, we chose to explore the same parameter range of the five parameters (α, $\mathcal{K}$, We, a, b) as for the rheological model. The results are presented in figures 4, 6, 8, 10 and 12. For each one of them, the width of the blocked band is represented as a function of two parameters, the other three being fixed. From a numerical point of view, let us remark that Figure 13, obtained for a looser grid, does not display significant differences: we have checked the grid used is fine enough for all simulations presented here.

In the (α, We) plane, the bands appear and grow as α is increased. And this happens earlier when We is smaller. In the ($\mathcal{K}$, We), bands appear when the value of the threshold $\mathcal{K}$ is increased, again this happens earlier when We is smaller. In the ($\mathcal{K}$, α), the bands again appear when the threshold is increased, and again when α is larger. The arguments rationalizing these observations are the same as in paragraph III B.

2. Comparison with the local rheological model

Comparing the figures of the previous paragraph and those of paragraph III B, we observe that the regions in

which blocked bands actually appeared in the 1D simulations are strictly included, as expected, in the regions authorized by the local rheological model.

However, the boundary of these regions do not coincide. Actually, a perfect mapping would require a very find adjustment of the profile of the initial conditions in order to explore the authorized zone for the shear bands up to its boundary. Figure 14 shows that modifying the amplitude and modulation in the initial stress can even lead to the disappearance of the blocked band.

V. CONCLUSION

As a conclusion, this model emphasizes the difference between the static and the dynamic flow thresholds, which determines the appearance of shear bands, for a material whose properties (as defined by rheological parameters) remain homogeneous. It is actually the tensorial character of the model which allows stress inhomogeneities, including in the initial conditions. Indeed, when the plastic flow starts, the material is free to deform in the third dimension (vorticity direction) and thus seems to *evolve*, when observed in 2D or 1D. This evolution can lead, locally, to a decrease of the shear stress to values below the static threshold σ_y. For an incompressible two-dimensional material, such behaviour would not be possible since the two eigenvalues of the stored deformation would be rigidly related.

Other materials which do not belong to the category of yield stress fluids could be analysed in the same way. For exampled, in entangled polymer solutions, transient shear bands are observed [42]. The fast band eventually spans the whole sample. The material has thus evolved as compared to the initial state. Since the average concentration cannot change, the evolution leading to this global fast band must affect the structure *via* a non-conserved order parameter. Measuring the radius of giration in the direction of vorticity could indicate whether ou analysis is relevant for this kind of fluid (taking a threshold stress equal to zero).

As a summary, without invoking an extra variable coupled to the flow, we show that a homogeneous 3D material may seem inhomogeneous when observed in 2D or 1D.

Appendix A: Direct method for obtaining the stationary state in the local rheological model

Let us start from the point $(\beta_1^y,\ \beta_2^y)$ and follow the plasticity threshold $W_y(B)=0$ until the stationarity condition is fulfilled. This condition can be expressed using the following observation: in the stationary regime, there is no plastic flow in the vorticity direction [3]. In other words, the third eigenvalue of tensor $\mathcal{G}(B)$ is zero:

$$g_3(\beta_1,\beta_2)=\mathcal{G}_3(\beta_1,\beta_2,\beta_3)=0, \tag{A1}$$

with $\beta_3=\frac{1}{\beta_1\beta_2}$. We thus directly obtain the dynamic threshold $(\beta_1^d,\ \beta_2^d)$ of the system. We then follow the same stationarity condition $g_3(\beta_1,\beta_2)=0$ until we reach the desired shear stress $\sigma_{12}=\sigma_y$. We thus directly obtain the stationary state $(\beta_1^{cc},\ \beta_2^{cc})$ that corresponds to the critical shear rate $\dot\gamma_c$. In practice, we follow the threshold curve using $\hat W_y(\beta_1,\beta_2)=W_y(\beta_1,\beta_2,\beta_3)=0$ (with $\beta_3=\frac{1}{\beta_1\beta_2}$) by integrating the following differential system:

$$\varepsilon_{W_y}\frac{\mathrm{d}\beta_1}{\mathrm{d}t} = \frac{\partial\hat W_y}{\partial\beta_2}=\frac{\partial W_y}{\partial\beta_2}-\frac{1}{\beta_1\beta_2^2}\frac{\partial W_y}{\partial\beta_3} \tag{A2}$$

$$-\varepsilon_{W_y}\frac{\mathrm{d}\beta_2}{\mathrm{d}t} = \frac{\partial\hat W_y}{\partial\beta_1}=\frac{\partial W_y}{\partial\beta_1}-\frac{1}{\beta_1^2\beta_2}\frac{\partial W_y}{\partial\beta_3} \tag{A3}$$

where the sign of $\varepsilon_{W_y}=\pm1$ is chosen in such a way as to follow the curve W_y in the desired direction. Similarly, we follow the curve of stationary states, $g_3(\beta_1,\beta_2)=\mathcal{G}_3(\beta_1,\beta_2,\beta_3)=0$ by integrating the following differential system:

$$\varepsilon_g\frac{\mathrm{d}\beta_2}{\mathrm{d}t} = \frac{\partial g}{\partial\beta_2}=\frac{\partial\mathcal{G}_3}{\partial\beta_2}-\frac{1}{\beta_1\beta_2^2}\frac{\partial\mathcal{G}_3}{\partial\beta_3} \tag{A4}$$

$$-\varepsilon_g\frac{\mathrm{d}\beta_2}{\mathrm{d}t} = \frac{\partial g_3}{\partial\beta_1}=\frac{\partial\mathcal{G}_3}{\partial\beta_1}-\frac{1}{\beta_1^2\beta_2}\frac{\partial\mathcal{G}_3}{\partial\beta_3} \tag{A5}$$

where the sign of $\varepsilon_g=\pm1$ is chosen in such a way as to follow the curve $g_3=0$ in the desired direction.

[1] L. Bécu, S. Manneville, and A. Colin. Spatiotemporal dynamics of wormlike micelles under shear. *Phys. Rev. Lett.*, 93:018301, 2004.

[2] S. Bénito. *Modélisation et simulation du comportement mécanique des milieux plastiques mous : mousses liquides et émulsions*. PhD thesis, Université Bordeaux 1, Bordeaux, FRANCE, 2009.

[3] S. Benito, C.-H Bruneau, T. Colin, C. Gay, and F. Molino. An elasto-visco-plastic model for immortal foams or emulsions. *Eur. Phys. J. E*, 25:225–251, 2008.

[4] J.-F. Berret. Rheology of wormlike micelles : equilibrium properties and shear banding transitions. *Molecular Gels*, 6:667–720, 2006.

[5] J.-F. Berret, D. C. Roux, and G. Porte. Isotropic-to-nematic transition in wormlike micelles under shear. *Europ. Phys. Journal E*, 4:1261–1279, 1994.

[6] A. Bertram. *Elasticity and Plasticity of large deformations*. Springer, Berlin, Heidelberg, New York, 2005.

[7] Lydéric Bocquet, Annie Colin, and Armand Ajdari. Kinetic theory of plastic flow in soft glassy materials. *Phys. Rev. Lett.*, 103(3):036001, Jul 2009.

[8] I. Cantat, S. Cohen-Addad, F. Elias, F. Graner, R. Höhler, O. Pitois, F. Rouyer, and A. Saint-Jalmes. *Les mousses - structure et dynamique*. Belin, Paris, 2010.

[9] G. Debrégeas, H. Tabuteau, and J.-M. di Meglio. Deformation and flow of a two-dimensional foam under continuous shear. *Phys. Rev. Lett.*, 87:178305, 2001.

[10] J. P. Decruppe, S. Lerouge, and J.-F. Berret. Insight in shear banding under transient flow. *Phys. Rev. E*, 63:022501, 1999.

[11] O. Diat, D. Roux, and F. Nallet. ''layering'' effect in a sheared lyotropic lamellar phase. *Phys. Rev. E*, 51(4):3296–3299, Apr 1995.

[12] Olivier Diat, Didier Roux, and Frédéric Nallet. Effect of shear on a lyotropic lamellar phase. *J. Phys. II France*, 3(9):1427–1452, sep 1993.

[13] E. Eiser, F. Molino, G. Porte, and O. Diat. Nonhomogeneous textures and banded flow in a soft cubic phase under shear. *Phys. Rev. E*, 61:6759–6764, 2000.

[14] E. Eiser, F. Molino, G. Porte, and X. Pithon. Flow in micellar cubic crystals. *Rheologica Acta*, 39:201–208, 2000.

[15] M. L. Falk and J. S. Langer. Dynamics of viscoplastic deformation in amorphous solids. *Phys. Rev. E*, 57:7192–7205, 1998.

[16] J. Goyon, A. Colin, G. Ovarlez, A. Ajdari, and L. Bocquet. Spatial cooperativity in soft glassy flows. *Nature*, 454:84–87, 2008.

[17] Keesha A. Hayes, Mark R. Buckley, Itai Cohen, and Lynden A. Archer. High resolution shear profile measurements in entangled polymers. *Phys. Rev. Lett.*, 101(21):218301, Nov 2008.

[18] R. Höhler and S. Cohen-Addad. Rheology of liquid foam. *J. Phys.: Condens. Matter*, 17:R1041–R1069, 2005.

[19] R. Höhler, S. Cohen-Addad, and V. Labiausse. Constitutive equation to describe the nonlinear elastic response of aqueous foams and concentrated emulsions. *J. Rheol.*, 48:679–690, 2004.

[20] E. Janiaud, D. Weaire, and S. Hutzler. Two-dimensional foam rheology with viscous drag. *Phys. Rev. Lett.*, 97(3):038302, Jul 2006.

[21] A. Kabla and G. Debrégeas. Local stress relaxation and shear banding in a dry foam under shear. *Phys. Rev. Lett.*, 90:258303, 2003.

[22] A. Kabla, J. Scheibert, and G. Debrégeas. Quasi-static rheology of foams. part 2. continuous shear flow. *J. Fluid. Mech.*, 587:45–72, 2007.

[23] Gijs Katgert, Matthias E. Möbius, and Martin van Hecke. Rate dependence and role of disorder in linearly sheared two-dimensional foams. *Phys. Rev. Lett.*, 101(5):058301, Jul 2008.

[24] Vincent J. Langlois, Stefan Hutzler, and Denis Weaire. Rheological properties of the soft-disk model of two-dimensional foams. *Phys. Rev. E*, 78(2):021401, Aug 2008.

[25] Marie Lenoble, Patrick Snabre, and Bernard Pouligny. The flow of a very concentrated slurry in a parallel-plate device: Influence of gravity. *Physics of Fluids*, 17(7):073303, 2005.

[26] S. Lerouge, M. Argentina, and J. P. Decruppe. Interface instability in shear-banding flow. *Phys. Rev. Lett.*, 96:088301, 2006.

[27] S. Lerouge and J.-F. Berret. Shear-induced transitions and instabilities in surfactant wormlike micelles. *Adv. Polym. Sci.*, 1:1–71, 2010.

[28] M. L. Manning, J. S. Langer, and J. M. Carlson. Strain localization in a shear transformation zone model for amorphous solids. *Phys. Rev. E*, 76(5):056106, Nov 2007.

[29] S. Marze, A. Saint-Jalmes, and D. Langevin. Protein and surfactant foams: linear rheology and dilatancy effects. *Colloids and Surface A*, 263:121–128, 2005.

[30] F. Molino, P. Rognon, and C. Gay. Note and calculations concerning elastic dilatancy in 2d glass-glass liquid foams. 2010.

[31] P.D. Olmsted and C.Y. Lu. Phase separation of rigid-rod suspensions in shear flow. *Phys. Rev. E*, 60(4):4397–4415, 1999.

[32] G. Picard, A. Ajdari, F. Lequeux, and L. Bocquet. Elastic consequences of a single plastic event : a step towards the microscopic modelling of the flow of yield stress fluids. *Eur. Phys. J. E*, 15:371, 2004.

[33] G. Picard, A. Ajdari, F. Lequeux, and L. Bocquet. Slow flows of yield stress fluids: complex spatiotemporal behavior within a simple elastoplastic model. *Phys. Rev. E*, 71:010501, 2005.

[34] G. Porte, J.-F. Berret, and J. Harden. Inhomogeneous flows of complex fluids: Mechanical instability versus non-equilibrium phase transition. *Europ. Phys. Journal E*, 7:459–472, 1997.

[35] C. Raufaste, S. J. Cox, P. Marmottant, and F. Graner. Discrete rearranging disordered patterns: prediction of elastic and plastic behaviour, and application to two-dimensional foams. *Phys. Rev. E*, 81:031404, 2010.

[36] O. Reynolds. *Philos. Mag.*, 20:469, 1985.

[37] F. Rioual, S. Hutzler, and D. Weaire. Elastic dilatancy in wet foams: a simple model. *Coll. Surf. A*, 263:117–120, 2005.

[38] P. Rognon, F. Molino, and C. Gay. Prediction of positive and negative elastic dilatancy in 2d and 3d liquid foams. *EPL (Europhysics Letters)*, 90:38001, 2010.

[39] J.-B. Salmon, S. Manneville, and A. Colin. Shear-banding in a lyotropic lamellar phase. part 1: Time-averaged velocity profiles. *Physical Review E*, 68:051503, 2003.

[40] J.-B. Salmon, S. Manneville, and A. Colin. Shear-banding in a lyotropic lamellar phase. part 2: Temporal fluctuations. *Physical Review E*, 68:051504, 2003.

[41] N.A. Spenley, M.E. Cates, and T.C. McLeish. Nonlinear rheology of wormlike micelles. *Phys. Rev. Lett.*, 71(6):939–942, 1993.

[42] Prashant Tapadia, Sham Ravindranath, and Shi-Qing Wang. Banding in entangled polymer fluids under oscillatory shearing. *Phys. Rev. Lett.*, 96(19):196001, May 2006.

[43] D. Weaire and S. Hutzler. *The Physics of Foams*. Oxford University Press, 1999.

[44] D. Weaire and S. Hutzler. Dilatancy in liquid foams. *Phil. Mag.*, 83:2747–2760, 2003.